

DETERMINATION OF FATIGUE CRACK PROPAGATION LIMIT CURVES FOR HIGH STRENGTH STEELS

János Lukács – Department of Mechanical Engineering, University of Miskolc, Hungary

ABSTRACT

There are different documents containing fatigue crack propagation limit or design curves and rules for the prediction of crack growth. The research work aimed to develop a new method for determination of fatigue crack propagation limit curves and determination of limit curves for different structural steels and high strength steels, and their welded joints, under different loading conditions, based on statistical analysis of test results and the Paris-Erdogan law. With the help of the characteristic values of threshold stress intensity factor range (ΔK_{th}), two constants of Paris-Erdogan law (C and n), fatigue fracture toughness (ΔK_{fc}) a new method can be proposed. Our testing results were compared with the testing results can be found in the literature. The limit curves calculated by the new method represent a compromise of rational risk (not the most disadvantageous case is considered) and striving for safety (uncertainty is known).

KEYWORDS

Limit curve, fatigue crack propagation, mode I, mixed mode I+II, Paris-Erdogan law, welded joints, statistical analysis, Weibull distribution.

INTRODUCTION

Reliability of a structural element having crack or crack-like defect under cyclic loading conditions is determined by the geometrical features of the structural element and the flaws, the loading conditions as well as the material resistance to fatigue crack propagation. There are different documents [1], [2], [3], standards and recommendations [4], [5], [6] containing fatigue crack propagation limit or design curves and rules for the prediction of crack growth [6], [7]. The background of the fatigue crack propagation limit curves and the calculations consist of two basic parts: statistical analysis of numerous experiments (fatigue crack propagation tests) and fatigue crack propagation law, frequently the Paris-Erdogan law [8].

The research work aimed

- (i) to develop a new method for determination of fatigue crack propagation limit curves based on statistical analysis of test results and the Paris-Erdogan law;
- (ii) determination of limit curves for different structural steels and high strength steels, and their welded joints, under mode I and mixed mode I+II loading conditions.

1. EXPERIMENTS

The tested structural steels and high strength steels, and their welded joints were as follows:

- micro-alloyed steel grade 37C and its welded joints by gas metal arc (GMA) welding using 100 % CO₂ gas and VIH-2 type filler material;

- micro-alloyed steel grade E420C and its welded joints by GMA welding using 80 % Ar + 20 % CO₂ gas mixture and Union K56 solid wire;
- high strength low alloyed (HSLA) steel grade X80TM and its welded joints by GMA welding using 82 % Ar + 18 % CO₂ gas mixture and Böhler X-90 IG solid wire;
- HSLA steel grade QStE690TM;
- HSLA steel grade XABO 1100.

The chemical composition, the measured (R_y , R_m , A_5 , Z) and calculated (R_y/R_m , $R_m * A_5$) mechanical properties and the impact toughness properties (KV at different temperatures) of the investigated base materials (bm) and weld metals (wm) are summarized in Table 1, Table 2 and Table 3, respectively.

Table 1 Chemical composition of the investigated structural steels and high strength steels, wt % (bm: base material; wm: weld metal)

Material	C	Si	Mn	P	S	Al	Nb	V	Cu
37C bm	0.15	0.38	0.89	0.029	0.016	0.016	0.021	0.023	–
VIH-2 wm	0.08-0.1	0.40-0.63	0.69-0.98	0.011-0.017	0.027-0.030	–	–	–	–
E420C bm ⁽¹⁾	0.18	0.46	1.44	0.027	0.013	0.025	0.035	0.045	0.08
Union K56 wm	0.10	1.10	1.70	≤0.020	≤0.020	≤0.020	–	≤0.020	–
X80TM bm ⁽²⁾	0.077	0.30	1.84	0.012	0.002	0.036	0.046	–	–
QStE690TM bm ⁽³⁾	0.08	0.29	1.75	0.011	0.002	0.041	0.04	0.061	0.33
Böhler X90-IG wm ⁽⁴⁾	0.10	0.60	1.75	–	–	–	–	–	–
XABO 1100 bm ⁽⁵⁾	0.16	0.29	0.98	0.012	0.0020	0.025	0.001	0.070	0.040

⁽¹⁾ Cr = 0.06 %, Ni = 0.03 %.

⁽²⁾ Ti = 0.018 %, N = 0.0051 %.

⁽³⁾ Cr = 0.037 %, Ni = 0.52 %, Mo = 0.32 %, Ti = 0.024 %.

⁽⁴⁾ Cr = 0.30 %, Ni = 2.5 %, Mo = 0.45 %.

⁽⁵⁾ Cr = 0.66 %, Ni = 1.93 %, Mo = 0.51 %, Ti = 0.001 %, N = 0.0049 %, B = 0.0002 %.

Table 2 Mechanical properties of the investigated structural steels and high strength steels (bm: base material; wm: weld metal)

Material	R_y ⁽¹⁾ N/mm ²	R_m N/mm ²	R_y/R_m –	A_5 %	$R_m * A_5$ N/mm ² * %	Z %
37C bm	270	405	0.666	33.5	13567	63.5
VIH-2 wm	410-485	535-585	0.766-0.829	22.0-24.8	≥11770	40.9-63.9
E420C bm	450	595	0.756	30.7	18266	–
Union K56 wm	≥500	560-720	0.694-0.893	≥22.0	≥12320	–
X80TM bm	540	625	0.864	25.1	15687	73.1
QStE690TM bm	780	850	0.918	18.3	15555	–
Böhler X90-IG wm	≥890	≥940	≈0.947	≥16.0	≥15040	–
XABO 1100 bm	1125	1339	0.840	11.0 ⁽²⁾	14729	–

⁽¹⁾ R_y means R_{eH} or $R_{p0.2}$.

⁽²⁾ For these material A_{97} .

Table 3 Impact properties of the investigated base materials (bm) and weld metals (wm)

Material	Impact toughness, KV, J, at testing temperature				
	20 °C	0 °C	-20°C	-40 °C	-60 °C
37C bm	–	>27	–	–	–
VIH-2 wm	–	46-80	29-61	–	–
E420C bm	–	>40	–	–	–
Union K56 wm	–	–	≥47	–	–
X80TM bm	–	–	≥243	–	128-208
QStE690TM bm	130	90	95	35	20
Böhler X90-IG wm	–	≥100	≥90	80	60
XABO 1100 bm	–	–	–	32	–

Compact tension (CT) and three point bending (TPB) specimens were tested for base materials and welded joints, while for testing of weld metal TPB type specimens were used. CT type specimens were cut from the sheets parallel and perpendicular to the rolling direction, so the directions of fatigue crack propagation were the same. For testing of weld metals cracks, which propagate parallel or perpendicular to the axis of the joint were also distinguished. Compact tension shear (CTS) specimens were used for tests under mixed mode I+II loading condition. The specimens were cut parallel to the rolling direction, so the cracks were propagated perpendicular to the rolling direction. Tests were carried out according to the ASTM prescription [9] by an universal electrohydraulic MTS testing machine. Experiments were performed by ΔK -decreasing and constant load amplitude methods, at room temperature, in air, following sinusoidal loading wave form. Stress ratio was constant ($R=0.1$), crack propagation was registered by compliance and/or optical method.

2. DETAILS OF INVESTIGATIONS ON XABO 1100 HSLA STEEL

CT specimens were tested under mode I loading condition, the notch or crack propagation directions were T-L and L-T. The crack size-number of cycle curves are shown in Fig. 1.

Fig. 1 Crack size-number of cycle curves from tested XABO 1100 specimens

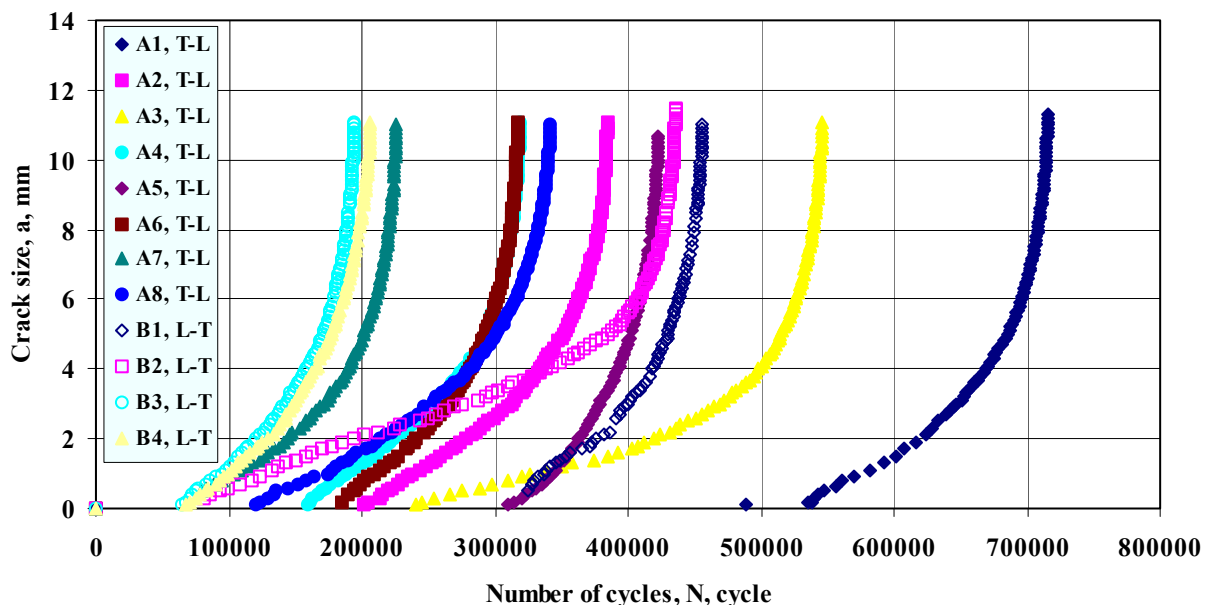


Fig. 2 shows the calculated kinetic diagrams using secant method and Table 4 summarizes the determined material properties (C and n, ΔK_{fc}) and correlation indexes.

Fig. 2 Kinetic diagrams of fatigue crack propagation from tested XABO 1100 specimens

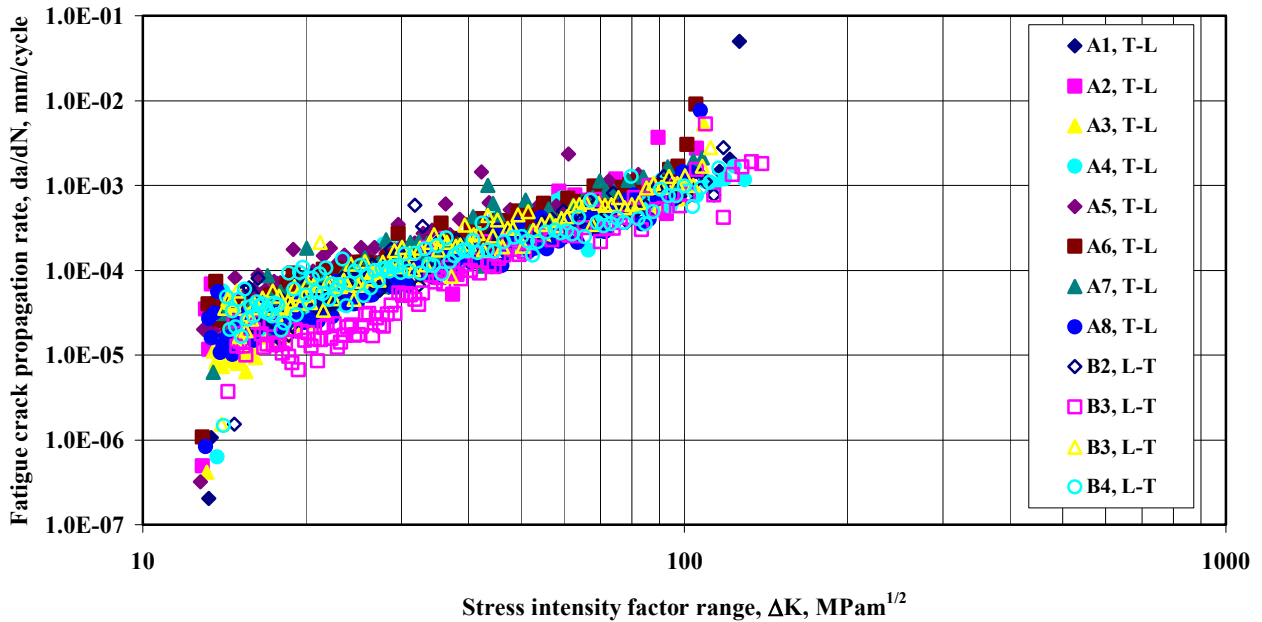


Table 4 Experimental results of fatigue crack propagation test measured on XABO 1100 steel

Specimen, orientation	C	n	ΔK_{fc}	Correlation index
	mm/cycle and	MPam ^{1/2}	MPam ^{1/2}	
A1, T-L	1.29 E-07	1.95	129.2	0.9693
A2, T-L	8.93 E-08	2.08	109.5	0.9568
A3, T-L	2.39 E-08	2.38	113.0	0.9666
A4, T-L	1.69 E-07	1.87	132.1	0.9653
A5, T-L	3.00 E-07	1.85	92.6	0.9319
A6, T-L	1.65 E-07	1.97	107.0	0.9735
A7, T-L	8.21 E-08	2.15	110.1	0.9584
A8, T-L	1.28 E-07	1.89	109.1	0.9586
B1, L-T	1.88 E-07	1.85	120.2	0.9286
B2, L-T	1.21 E-08	2.42	142.1	0.9633
B3, L-T	1.90 E-07	1.89	114.0	0.9617
B4, L-T	3.54 E-07	1.67	118.0	0.9466

3. DETERMINATION OF FATIGUE DESIGN LIMIT CURVES

Determination of fatigue crack propagation design curves consists of six steps.

First step: determination of measuring values. Values of threshold stress intensity factor range (ΔK_{th}) and two parameters of Paris-Erdogan law (C and n) were calculated according to ASTM prescriptions [9]. Fatigue crack growth was determined by secant method or seven point incremental polynomial method. Values of fatigue fracture toughness (ΔK_{fc}) were calculated from crack size determined on the fracture surface of the specimens by the means of stereo-microscope.

Second step: sorting measured values into statistical samples. On the basis of calculated test results, mathematical-statistical samples were examined for each testing groups. As its method, Wilcoxon-probe was applied [10], furthermore statistical parameters of the samples were calculated. The mathematical-statistical samples of tested base materials and their welded joints are summarized in Table 5.

Table 5 Mathematical-statistical samples of tested steels and their parameters
(bm: base material; wj: welded joint)

Material	Orientation	Parameter	Element number of sample	Average	Standard deviation	Standard deviation coefficient
37 C bm	T-L, L-T	ΔK_{th}	9	7.69	1.220	0.1587
	T-L	n	37	3.74	0.534	0.1430
	T-L	ΔK_{fc}	34	66.03	5.943	0.0900
	L-T	n	33	3.45	0.311	0.0901
	L-T	ΔK_{fc}	28	58.67	3.560	0.0607
37C wj	all ⁽¹⁾	n	36	4.11	0.747	0.1818
	all ⁽²⁾	ΔK_{fc}	14	76.23	5.603	0.0735
E420 C bm	T-L, L-T	ΔK_{th}	7	5.72	1.038	0.1812
	T-L	n	32	2.58	0.182	0.0706
	T-L	ΔK_{fc}	27	101.52	5.302	0.0522
	L-T	n	7	2.42	0.191	0.0788
	L-T	ΔK_{fc}	5	94.43	0.964	0.0102
E 420 C wj	all ⁽²⁾	n	17	3.603	0.568	0.1577
	all ⁽²⁾	ΔK_{fc}	15	113.9	9.197	0.0808
X80TM bm	all ⁽³⁾	n	26	2.49	0.561	0.2251
	T-L, L-T	ΔK_{fc}	10	136.57	3.627	0.0266
X80TM wj	2-3	n	18	2.45	0.831	0.3386
QStE690TM bm	all ⁽³⁾	n	16	2.39	0.495	0.2070
QStE690TM bm ^{(4), (5)}	T-L, L-T	n	10	2.80	0.444	0.1588
XABO 1100 bm	<i>T-L</i>	<i>n</i>	8	<i>2.02</i>	<i>0.180</i>	<i>0.0890</i>
	<i>T-L</i>	ΔK_{fc}	8	<i>112.82</i>	<i>12.621</i>	<i>0.1119</i>
	<i>L-T</i>	<i>n</i>	4	<i>1.96</i>	<i>0.323</i>	<i>0.1649</i>
	<i>L-T</i>	ΔK_{fc}	4	<i>123.57</i>	<i>12.614</i>	<i>0.1021</i>
	T-L, L-T	n	12	2.00	0.223	0.1117
	T-L, L-T	ΔK_{fc}	12	116.41	13.144	0.1129

⁽¹⁾ 2-3, T-L/1-2, T-L/2-1, L-T/1-2, L-T/2-1.

⁽²⁾ T-L/1-2, T-L/2-1, L-T/1-2, L-T/2-1.

⁽³⁾ T-L, L-T, L-S.

⁽⁴⁾ Under mixed mode I+II loading condition.

⁽⁵⁾ ΔK should be replaced by ΔK_{eff} .

Standard deviation coefficients (standard deviation/average) in Table 5 are generally less than 0.2, which means reliable and reproducible testing and data processing methods.

Third step: selection of the distribution function. Afterwards it was examined, what kind of distribution functions can be used for describing the samples. For this aim, Shapiro-Wilk, Kolmogorov, Kolmogorov-Smirnov and χ^2 - probe were used at a level of significance $\varepsilon=0.05$ [10]. It was concluded, that Weibull-distribution is the only function suitable for describing all the samples.

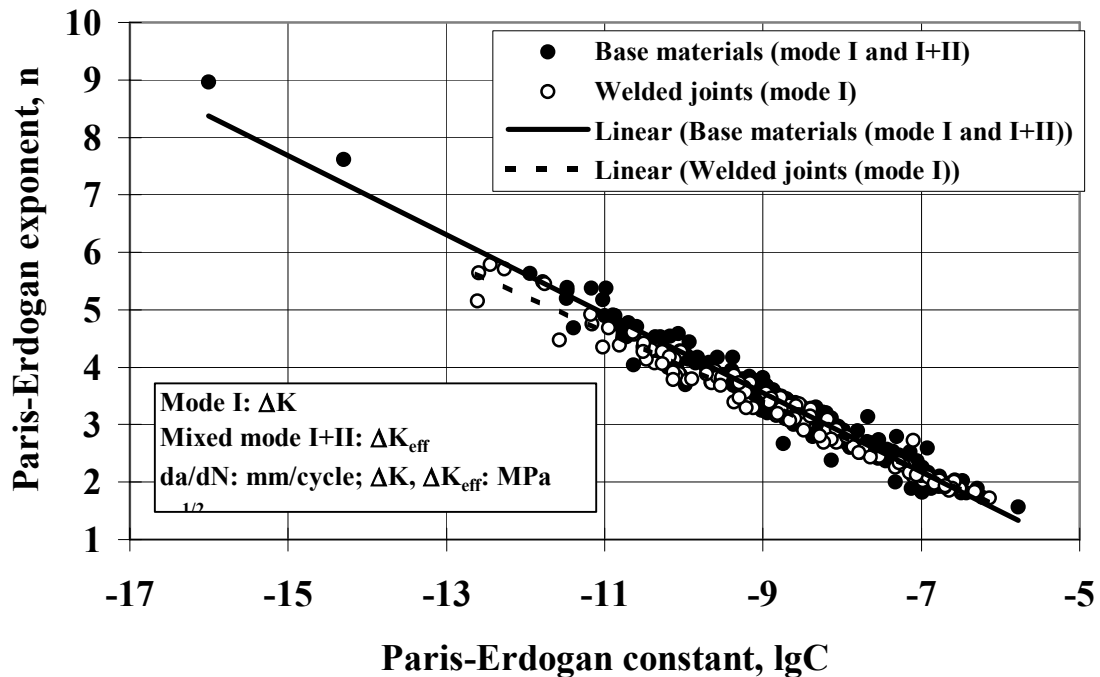
Fourth step: calculation of the parameters of the distribution functions. Parameters of three parameter Weibull-distribution function were calculated for all the samples:

$$F(x) = 1 - \exp \left[- \left(\frac{x - N_0}{\beta} \right)^{1/\alpha} \right]. \quad (1)$$

Fifth step: selection of the characteristic values of the distribution functions. Based on the calculated distribution functions, considering their influencing effect on life-time, characteristic values of ΔK_{th} , n and ΔK_{fc} , were selected. With the help of these values a new method can be proposed for determination of fatigue crack propagation limit curves:

- the threshold stress intensity factor range, ΔK_{th} , is that value which belongs to the 95% probability of the Weibull-distribution function;
- the exponent of the Paris-Erdogan law, n , is that value belonging the 5% probability of Weibull-distribution function;
- the constant of the Paris-Erdogan law, C , is calculated on the basis of the correlation between C and n (Fig. 3);

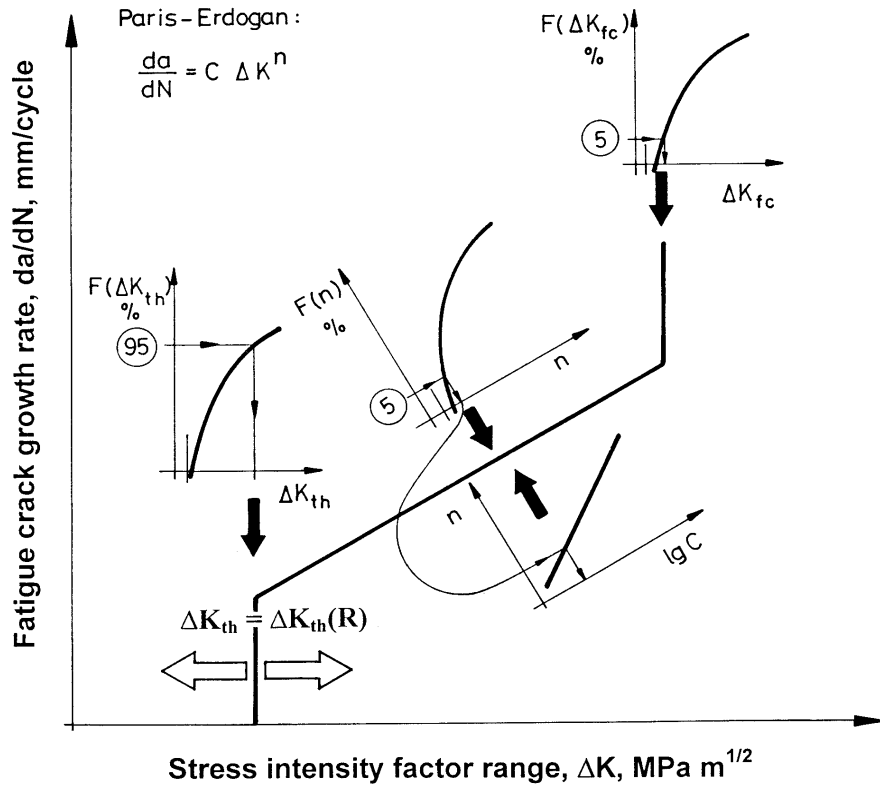
Fig. 3 Connection between the exponent (n) and the constant (C) of Paris-Erdogan law



- the critical value of the stress intensity factor range or fatigue fracture toughness, ΔK_{fc} , is that value which belongs to the 5% probability of the Weibull-distribution function.

Fig. 4 shows the proposed method schematically.

Fig. 4 Schematic presentation of the proposed new method for determination of fatigue crack propagation limit curves



Sixth step: calculation of the parameters of the fatigue crack propagation limit curves. The details of fatigue crack propagation limit curves determined for steels and high strength steels can be found in the Table 6, the curves are presented in Fig. 5.

Table 6 Details of determined fatigue crack propagation limit curves

Material	ΔK_{th} $MPam^{1/2}$	C		ΔK_{fc} $MPam^{1/2}$
		n	$MPam^{1/2}$ and mm/cycle	
37C base material	10.4	2.98	8.22E-09	53
37C welded joint	— ^{(1), (2)}	3.16	2.42E-09	70
E420C base material	8.0	2.26	9.78E-08	92
E420C welded joint	— ^{(1), (3)}	2.74	1.16E-08	101
X80TM base material	—	1.78	3.74E-07	129
X80TM welded joint	— ⁽¹⁾	1.86	3.13E-07	—
QStE690TM base material	—	1.82	3.27E-07	—
QStE690TM base material ^{(4), (5)}	—	2.15	1.09E-07	—
XABO 1100 base material	—	1.76	4.00E-07	104

⁽¹⁾ It can be derived from data concerning to the base metal after the evaluation of characteristic and assessment of magnitude of residual stresses.

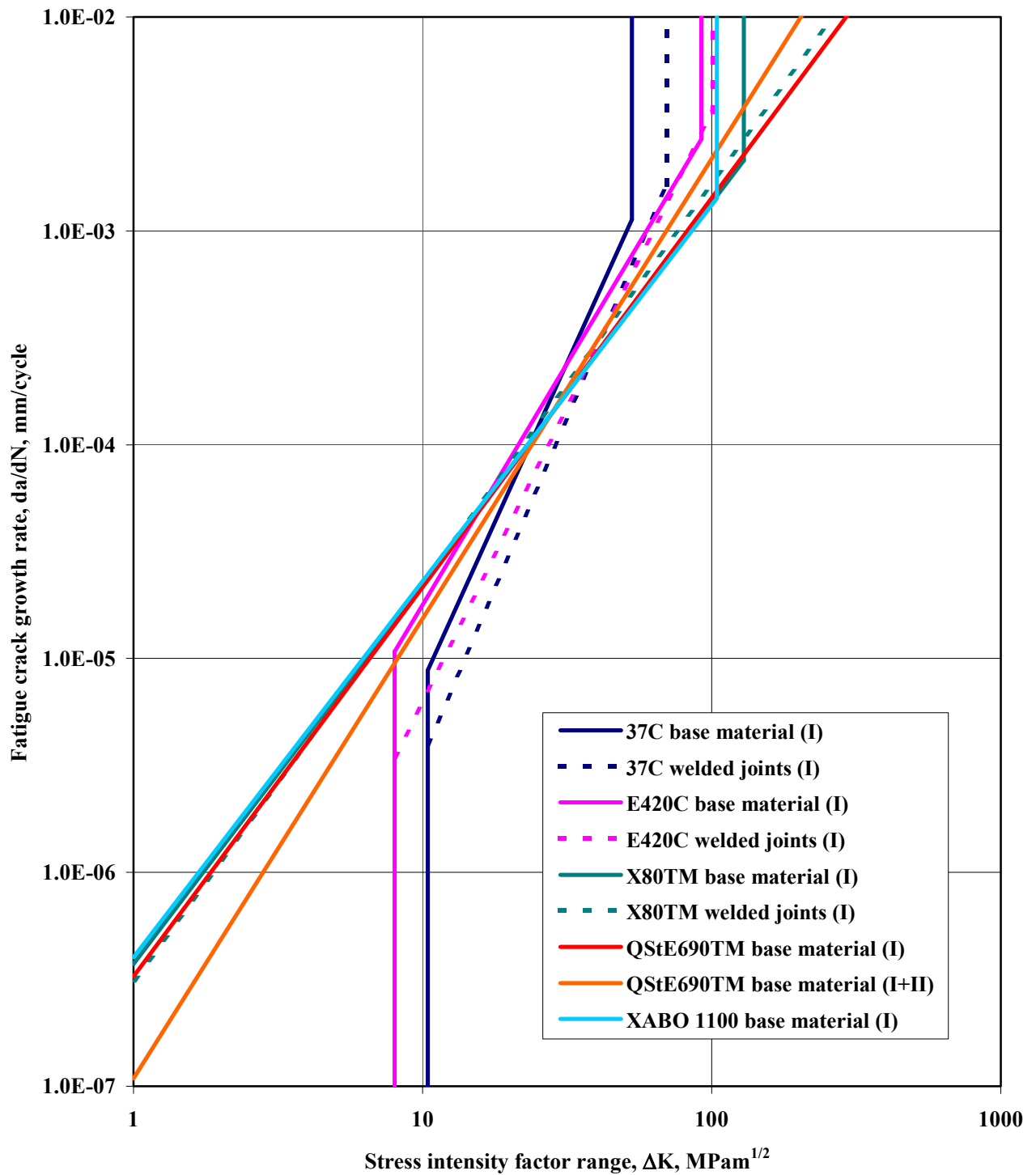
⁽²⁾ Average value of 16 tests under compressive residual stress: $\Delta K_{th} = 16.9 MPam^{1/2}$.

⁽³⁾ Average value of 4 tests under compressive residual stress: $\Delta K_{th} = 16.3 MPam^{1/2}$.

⁽⁴⁾ Under mixed mode I+II loading condition.

⁽⁵⁾ ΔK should be replaced by ΔK_{eff} .

Fig. 5 Fatigue design limit curves for micro-alloyed and HSLA steels and their welded joints



4. DISCUSSION

For the investigated steels and their welded joints both the threshold stress intensity factor range (ΔK_{th}) and the exponent of the Paris-Erdogan law (n) decrease with the increase of the strength of steel, while the fatigue fracture toughness (ΔK_{fc}) increases.

For the investigated steels both the exponent of the Paris-Erdogan law (n) and the fatigue fracture toughness (ΔK_{fc}) for welded joints are higher than those of base materials.

The proposed method is suitable for determination of fatigue crack propagation design curves under mixed mode I+II loading condition. For this case stress intensity factor range (ΔK) should be replaced by effective stress intensity factor range (ΔK_{eff}).

The design curves of welded joints in the near threshold region are open. The threshold stress intensity factor range, ΔK_{th} , must be reduce by tensile residual stress field and may be increase by compressive residual stress field (e.g. welding residual stresses).

The calculated fatigue crack propagation limit curves of steels locate among the design curves determined by various procedures.

Table 7 summarizes our measured average data and measured individual data can be found in the literature [11]. It can be concluded that our average values are in harmony with the individual values.

Table 7 Comparison of measured data with data from the literature

Material	R_y	R_m	ΔK_{th}	n	ΔK_{fc}
	N/mm ²	N/mm ²	MPam ^{1/2}	MPam ^{1/2} and mm/cycle	MPam ^{1/2}
37C	270	405	7.69	3.60	62.70
St38b-2	280	440	5.5	3.7	45
E420C	450	595	5.72	2.55	100.41
H60-3	500	630	5.9	3.8	50
X80TM	540	625	–	2.49	136.57
H75-3	600-680	–	4.3-5.2	2.5-2.7	70-75
QStE690TM	780	850		2.39	–
N-A-XTRA 70	810	850	2.7	2.7	88
XABO 1100	1125	1339	–	2.00	116.41

5. CONCLUSIONS

Based on the results of our experimental tests, evaluated samples and data can be found in the literature the following conclusions can be drawn.

- (i) The proposed method can be generally applied for determination of fatigue crack propagation limit curves for steels and high strength steels, and their welded joints under mode I and mixed mode I+II loading conditions. Additional information of applications of the proposed method for metallic (e.g. pressure vessel steels, aluminium alloys, austempered ductile iron) and non-metallic (e.g. silicon nitride ceramics, polymers, reinforced polymer matrix composites) materials see in our earlier works in the literature [12], [13], [14], [15], [16].
- (ii) The limit curves represent a compromise of rational risk (not the most disadvantageous case is considered) and striving for safety (uncertainty is known).
- (iii) Based on the determined fatigue design limit curves integrity assessment calculations can be done for operating structural elements and structures having cracks or crack-like defects.

ACKNOWLEDGEMENTS

Author wishes to acknowledge the assistance given by the National Scientific Research Foundation (OTKA F 4418, OTKA T 022020 and OTKA T 034503) and the Hungarian Academy of Sciences (Bolyai János Scholarship) for supporting the research.

REFERENCES

- 1) R. J. ALLEN, G. S. BOOTH and T. JUTLA, *Fat. Fract. Eng. Mater. Struct.* 11, (1988), p. 45.
- 2) R. J. ALLEN, G. S. BOOTH and T. JUTLA, *Fat. Fract. Eng. Mater. Struct.* 11, (1988), p. 71.
- 3) A. OHTA et al., *Trans. Jap. Weld. Soc.* 20, (1989), p. 17.
- 4) Merkblatt DVS 2401 Teil 1, Bruchmechanische Bewertung von Fehlern in Schweissverbindungen. Grundlagen und Vorgehensweise. (Oktober 1982).
- 5) Det norske Veritas, Classification Notes, Note No. 30.2, Fatigue strength analysis for mobile offshore units. (August 1984).
- 6) BS 7910, Guide on methods for assessing the acceptability of flaws in fusion welded structures (1999)
- 7) Merkblatt DVS 2401 Teil 2, Bruchmechanische Bewertung von Fehlern in Schweissverbindungen. Praktische Anwendung. (April 1989).
- 8) P. PARIS and F. ERDOGAN, *Journ. Bas. Eng.*, *Trans. ASME.* (1963), p. 528.
- 9) ASTM E 647, Standard test method for measurement of fatigue crack growth rates. (1988).
- 10) D. B. OWEN, Handbook of statistical tables. Vychislitel'nyjj Centr AN SSSR, Moskva (1973). (In Russian).
- 11) H. BLUMENAUER (Ed.), Bruchmechanische Werkstoffcharakterisierung. Deutscher Verlag für Grundstoffindustrie, Leipzig (1991), p. 135.
- 12) J. LUKÁCS, *Publ. Univ. Miskolc, Series C. Mech. Engng.* 46, (1996) p. 77.
- 13) J. LUKÁCS, Third International Pipeline Technology Conference. R. DENYS, (Ed.). Elsevier Science B. V. 2, (2000), p. 127.
- 14) I. TÖRÖK, *Publ. Univ. Miskolc, Series. C, Mech. Engng.* 46 (1996) p. 33.
- 15) J. LUKÁCS, Proceedings of the Eighth International Fatigue Congress (FATIGUE 2002), Stockholm (2002), EMAS, West Midlands (2002), p. 1179.
- 16) J. LUKÁCS, *Materials Science Forum*, 414-415, (2003) p. 31.